SPEED CONTROL OF LINEAR INDUCTION MOTOR USING DTFC METHOD CONSIDERING END-EFFECT PHENOMENON

H. Shadabi [1]   A. Rahnama Sadat [1]   A. Pashaei [2]   M.B.B. Sharifian [1]

1. Faculty of Electrical and Computer Engineering, University of Tabriz, Tabriz, Iran
h.shabai91@ms.tabrizu.ac.ir, a.r.sadat@ieee.org, sharifian@tabrizu.ac.ir
2. Department of Electrical and Electronic Engineering, Faculty of Engineering, Gazi University, Ankara, Turkey
ali.pashaei@gazi.edu.tr

Abstract- In this paper the speed control method of LIM, which lead to optimal control characteristic of motor such as thrust, flux and current, is proposed. The performance of the proposed DTFC method is analyzed with considering end-effect. DTFC is one of the improved control methods which employ several PI controllers. Proper adjustment of coefficients of the PI controller plays an important role in the satisfactory performance of control system that are determined using MATLAB optimization functions. The obtained results show that the DTFC method considering end-effect has led to a considerable reduction in the FORCER flux and thrust ripple near to 0.8%. The most important feature of DTFC method is its performance robustness against the end-effect phenomenon.

Keywords: Direct Thrust Control, Indirect Vector Control, Linear Induction Motor, End Effect.

I. INTRODUCTION

Linear electric motors (LEMs) belong to the group of special electrical machines. Main applications of these machines are in high-speed ground transportation, sliding doors, flexible manufacturing systems, robotic systems, etc. [1]. In a linear induction motor (LIM), the primary winding corresponds to the stator winding of a rotary induction Motor (RIM), while the secondary corresponds to the rotor. Normally, the secondary part of a LIM is made of aluminum and steel plates. As the primary moves, a new flux is continuously developed at the entry of the primary yoke, while existing flux disappears at the exit side.

Sudden generation and disappearance of the penetrating field causes eddy currents in the secondary plate. This eddy current affects the air gap flux profile in the longitudinal direction. The losses, as well as the flux-profile attenuation, become severer as the speed increases. Such a phenomena is called 'End Effect' of LIM [2]. So, the End Effects should be considered in both the modeling and controlling of LIM in order to achieve speed or thrust tracking.

A current control type vector control is generally used as a control method of LIM [2, 3]. The control scheme requires rotor position detector, the rotating coordinate transformation, and the current controller of which PI control is general, which needs the gain tuning. As a result, the controller configuration becomes complicated.

In recent years, direct thrust control (DTC) is preferable to give a fast and good dynamic thrust response in the small and medium power range applications. This control method is different in terms of the operation principle from the field oriented control (FOC) or the vector control technique. As the vector control is a method based on primer current control in the synchronous reference frame, DTC is a method based on primer flux control in the stationary reference frame [4, 5].

DTC structure is very simple in comparison with the conventional vector control and is characterized by fast dynamic response and low thrust ripple. Direct thrust control does not require a rotor position detector and the current controller in the rotating coordinate system. Thus, position sensorless control can be realized easily. DTC-based drives do not require the coordinate transformation between stationary frame and synchronous frame and the inverter is directly controlled by the inverter switching states selected using switching table. Thus, neither current controllers nor pulse-width modulation (PWM) modulator is needed [6]. However, the main disadvantage of DTC is the need for high sampling rate and variable switching frequency resulting from hysteresis based control loops. [7].

In addition, many studies of DTC in linear induction motor drives are performed [1, 3]. Linear motors have been examined with three-phase moving magnetic field models and insufficiently-research parts of the problem were interpreted as different models in the literature has been evaluated. Polar step-change on the moving area was modeled with variation of magnetic flux. The rotor and stator magnetic flux change was demonstrated graphically and envelops during in different times calculated theoretically [8].

Equivalent circuit modeling of a linear induction motor is more complicated than a rotary induction motor because of the existence of the End Effect. In a rotary induction motor, an accurate equivalent circuit model is obtained due to its pole-by-pole symmetry. In the LIM because of the existence of the End Effects, electrical conditions vary at the entry and exit point, so the pole symmetry argument is not maintained. Most of the existing models of LIMs, which have been derived in recent literatures, cannot be directly applied for the vector control because of their dependency on field theory. Thus, an accurate equivalent circuit model of LIMs is essential for vector control drive [10].

To eliminate disadvantage of conventional DTC such as high ripple of torque and flux in low speed, the new control method has been proposed. In this method the frequency of inverter switching has been increased. The proposed control method, controls inverter switches directly by means of predictive capability [11]. There are several techniques for modeling of LIM in rotating reference frame, which help to simulate precisely [12]. The model of LIM with considering end effect had been proposed in [13].

In this paper, first the dynamic model of the linear induction motor with including End Effects is represented. By using direct thrust control, position sensorless drive is available in linear metro and that can be used as a fail-safe function of the vector control when position sensor broke. Proper adjustment of coefficients of the PI controller plays an important role in the satisfactory performance of control system. To adjust the coefficients of PI controllers FINDLIMITS function and COST function which are two kinds of optimization functions of MATLAB software are used. In addition, the simulation result at starting and accelerating in both control schemes is discussed and has been shown by employed DTFC control methods. Control characteristics have been improved and End Effect does not have any influence on the control of the thrust and the speed.

II. DYNAMIC MODEL OF LINEAR INDUCTION MOTOR

A mathematical model of three-phase, two-pole permanent-magnet synchronous motors should be developed. Three-phase, two-pole permanent-magnet synchronous motor is illustrated in Figure 1.

A. Motor Modeling

To obtain a suitable LIM equivalent circuit, we must quantify the end effects during entry and exit from the secondary [14]. Figure 1 shows the fluxes induced by moving part which called End Effect. Therefore, the End Effect is modeled by $f(Q)$ which is represented by:

$$f(Q) = \frac{1 - e^{-Q}}{Q} \qquad (1)$$

where, Q is a factor related to not only the primary length but also the machine velocity:

$$Q = \frac{DR_r}{L_r v} \qquad (2)$$

where, R_r and L_r are rotor resistance and inductance respectively, v is the linear primary speed in m/s, D is the primary length in meters. It can be seen in Equation (2) that the Q factor is inversely dependent on the velocity. I.e. for a zero velocity the End Effects can be neglected ($Q = \infty$, $f(Q) = 0$). As the velocity increases, the end-effects increase and this causes a reduction of the magnetization current of LIM. This effect may be quantified by modifying the magnetization inductance as follows:

$$L_m' = L_m\left(1 - f(Q)\right) \qquad (3)$$

On the other hand, ohmic losses occurring with the increase of the eddy currents induced at the entry and exit ends of the secondary must be taken into consideration when the equivalent circuit is created. So, a resistance inserts in series with the inductance in the magnetization branch of the equivalent electrical circuit. This resistance represents the ohmic losses produced by the eddy currents and it is described as the product of the secondary resistance R_r by the $f(Q)$ factor:

$$R_{eddy} = R_r f(Q) \qquad (4)$$

The equivalent circuit of the LIM is represented as shown in Figure 2. This circuit is on a per phase basis. At low speeds, there is no difference between the equivalent circuits of LIM and RIM. However, if the primary moves, the equivalent circuit of RIM is not good for LIM because of the existence of the end effect. In order to develop the dynamic analysis and model-based control algorithms of LIM, the equivalent model must be expressed in d-q model as shown in Figure 3 and Figure 4 respectively.
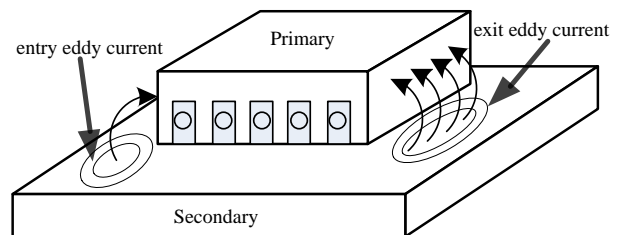

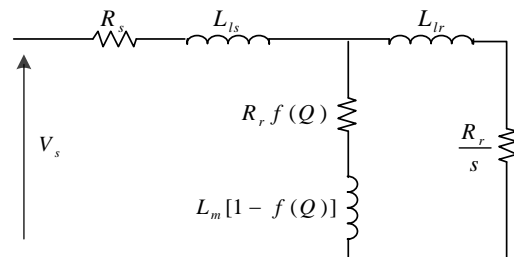Figure 1. End-effect conception in LIM
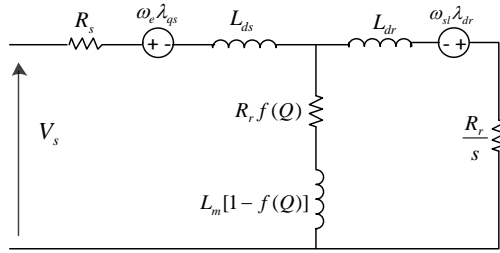

Figure 2. Per-phase LIM equivalent circuit

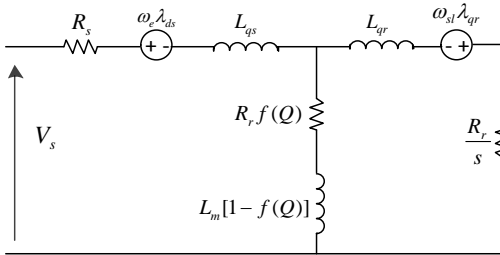Figure 3. The d-axis equivalent circuit

Figure 4. The q-axis equivalent circuit

From the d-q equivalent circuit of LIM, the primary and secondary voltage equations are given as follows:

$$V_{ds} = R_s i_{ds} + R_r f\left(Q\right)\left(i_{ds} + i_{dr}\right) + p\lambda_{ds} - \omega_e \lambda_{qs} \tag{5}$$

$$V_{qs} = R_s i_{qs} + p\lambda_{qs} + \omega_e \lambda_{ds} \tag{6}$$

$$V_{dr} = R_s i_{dr} + p\lambda_{ds} - \left(\omega_e - \omega_r\right)\lambda_{qs} \tag{7}$$

$$V_{qr} = R_r i_{qr} + p\lambda_{qr} + \left(\omega_e - \omega_r\right)\lambda_{dr} \tag{8}$$

$$\lambda_{ds} = L_{ls} i_{ds} + L_m\left(1 - f\left(Q\right)\right)\left(i_{ds} + i_{dr}\right) \tag{9}$$

$$\lambda_{qs} = L_{ls} i_{qs} + L_m\left(i_{ds} + i_{dr}\right) \tag{10}$$

$$\lambda_{dr} = L_{lr} i_{qr} + L_m\left(1 - f\left(Q\right)\right)\left(i_{ds} + i_{dr}\right) \tag{11}$$

$$\lambda_{qr} = L_{lr} i_{qr} + L_m\left(i_{ds} + i_{dr}\right) \tag{12}$$

where R_s is the stator resistance, i_{ds}, i_{dr} and i_{qs}, i_{qr} are the stator and rotor currents in d-q reference frame respectively, L_{ls}, L_{lr} are stator and rotor leakage fluxes, λ_{ds}, λ_{dr} and λ_{qs}, λ_{qr} are stator and rotor fluxes in d-q reference frame respectively.

The thrust force and the motion equation are expressed as Equations (13) and (14), respectively:

$$F_e = \frac{3}{2}\frac{\pi}{\tau_p}\frac{p}{2}\left(\lambda_{dr} i_{qs} - \lambda_{qr} i_{ds}\right) \tag{13}$$

$$F_e = m\frac{dv}{dt} + Bv + F_L \tag{14}$$

where, p is the poles number, τ_p is the pole pitch, F_L is the load thrust force, B is the viscous friction coefficient of the LIM, m is the mass of the LIM.

III. PROPOSED DIRECT THRUST FORCE CONTROL FOR LINEAR INDUCTION MOTOR

Direct thrust force control is hysteresis control of the forcer flux and thrust, using the flux linkage estimated by the command voltage and the armature current on the d-q coordinate. Output stator voltage vector is directly selected according to vector selection table and output of the hysteresis controllers.

The difference between the reference value and the actual force and flux, which called the error signal, is input of the hysteresis controller. To control the thrust and flux, dual-band and single- band hysteresis controller are used respectively. In these controllers, the favorable bandwidth of the force and flux error has been determined, by considering the thrust and flux error signal, command to increase or decrease the force and flux is given based on the switching table.

At this stage by knowing the current position vectors of force and flux, depending on either increase or decrease the amount of force or flux, the optimum voltage vector were selected from switching table (Lookup-Table) and is sent to converter (Inverter) to apply to the motor. So, thrust and forcer flux linkage are controlled directly by selecting an appropriate stator voltage vector. Optimum switching sequence in inverter is expressed in Table 1. Figure 6 shows a block diagram of DTFC. Flux linkage is estimated by the following equations:

$$\lambda_{ds} = \int\left(v_{ds} - R_s i_{ds} - R_r f\left(Q\right) i_{ds}\right)dt \tag{15}$$

$$\lambda_{qs} = \int\left(v_{qs} - R_s i_{qs}\right)dt \tag{16}$$

$$\left|\lambda_s\right| = \sqrt{\left(\lambda_{ds}^2 + \lambda_{qs}^2\right)} \tag{17}$$

where, λ_{ds} and λ_{qs} are the estimated flux linkage on the d-q coordinate, v_{ds} and v_{qs} are voltage commands on the d-q coordinate, i_{ds} and i_{qs} are the estimated currents on the d-q coordinate, λ_s is the stator flux linkage, and R_s is the stator resistance. The position of primer flux is denoted by θ_λ and given by Equation (18):

$$\theta_\lambda = \tan^{-1}\left(\frac{\lambda_{qs}}{\lambda_{ds}}\right) \tag{18}$$

The thrust value is estimated as follows:

$$F_e = \frac{3}{2}\frac{\pi}{\tau_p}\frac{p}{2}\left(\lambda_{ds} i_{qs} - \lambda_{qs} i_{ds}\right) \tag{19}$$

Figure 7 shows simple expression model of a three-phase inverter and a motor. The relation between voltage vector and flux control area is depicted in Figure 8.
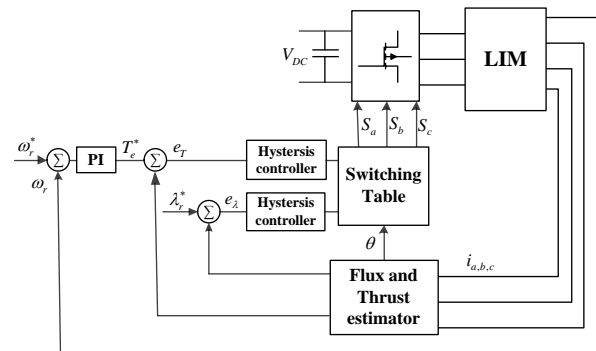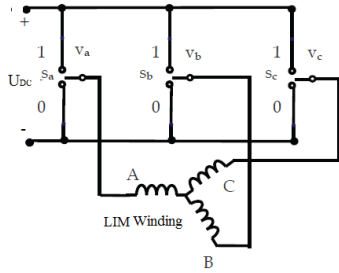

Figure 6. A block diagram of DTFC

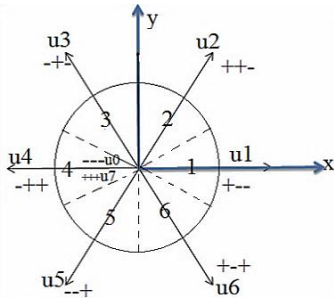Figure 7. Simple expression diagram of a three-phase inverter - LIM

Figure 8. Relation between voltage vector and flux control section

Each switches SW_u, SW_v and SW_w takes either state of "1" or "0". Thus, the number of switching mode of three-phase inverter is eight. For example, in order to have u_1, in output switch states of SW_u, SW_v and SW_w take "1", "0" and "0" respectively. As shown in Figure 6, hysteresis comparators give the torque and flux-linkage error state to vector selection table; and then, appropriate stator voltage vector is selected according to the voltage vector selection table shown in Table 1.

Table 1. Vector selection table

		$\theta(1)$	$\theta(2)$	$\theta(3)$	$\theta(4)$	$\theta(5)$	$\theta(6)$
$e_{\Phi=1}$	$e_F=1$	2	3	4	5	6	1
	$e_F=0$	0	0	0	0	0	0
	$e_F=-1$	6	1	2	3	4	5
$e_{\Phi=0}$	$e_F=1$	3	4	5	6	1	2
	$e_F=0$	0	0	0	0	0	0
	$e_F=-1$	5	6	1	2	3	4

According to above analysis, we obtain a flux controller and speed controller from Equations (1) to (8) as follow:

$$i^*_{qs} = \frac{4\tau}{3p\pi} \frac{F^*}{\lambda^*_{dr}} \frac{L_r - L_m f(Q)}{L_m(1 - f(Q))} \tag{20}$$

$$i^*_{ds} = \frac{1}{L_m}(1 + T_r p)\lambda^*_{dr} \tag{21}$$

From Equation (4) we can obtain the slip frequency:

$$\omega_{sl} = \frac{1}{T_r} \frac{L_m}{\lambda_{dr}} i_{qs} \tag{22}$$

As mentioned, the stator currents of the linear induction machine are separated into flux- and thrust-producing components by utilizing transformation to the d-q coordinate system, whose direct axis (d) is aligned with the rotor flux space vector. If the d-axis primary current (flux current component) is kept constant, so the electromagnetic force is directly proportional to q-axis current. By using vector control technique, the thrust that is shown in Equation (13) can be calculated by the following equations:

$$F_e = \frac{3}{2} \frac{\pi}{\tau_p} \frac{p}{2}(\lambda_{dr} i_{qs}) \tag{23}$$

IV. OPTIMAL CALCULATION OF PI COEFFICIENT

To improve the performance of PI controllers, different method such as fuzzy logic techniques and genetic algorithm are used. In this section, coefficients of the controller are determined using an optimization function. Advantages of this method are simplicity and lack of need for additional parameters. The first step is to determine the objective function. Regarding the objectives of this study, the reduction of stator flux ripple, torque ripple and the speed error rate are importance. By controlling the torque ripple, speed ripple is also improved. Hence, the torque ripple and speed error have been considered in objective function. Since three PI are used in control system and the main goal of this study is PMSM speed control the objective function expressed as follows:

$$f\left(k_{p_j}, k_{I_j}\right) = \left|\omega_{ref} - \omega_{act}\right|, j = 1, 2, 3 \tag{24}$$

$$L_{b_j} < k_{p_j}, k_{I_j} < U_{b_j} \tag{25}$$

where, L_b and U_b are upper and lower bounds for the coefficients in the defined range.

Two functions of COST and FINDLIMITS are used as main optimization functions. A schematic of the system determines the coefficients alongside the control system block diagram are shown in Fig. 5. The maximum number of simulations repeat, the range of variables coefficients and convergence interval are given as inputs to the system. FINDLIMITS function applies defined boundary constraints on the system during the computation.

Then, with an initial guess that according to bounds of the specified range is defined, the system starts calculation. For each simulation repeat, the motor response is compared with the reference, point- to -point, and the average error is calculated for the entire simulation period. If the error is not within the interval convergence, the simulation is repeated. A COST function performs convergent examining. These two functions with programs written in a m file, determine the coefficients of controllers.
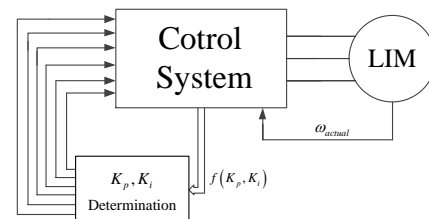

Figure 9. Optimal PI Coefficients Determination

V. SIMULATION RESULTS

In this section simulation results to verify the capability and feasibility of proposed control method are shown. The Main aid of this paper is speed control of LIM. For this purpose, the reference value of LIM speed is selected 8 m/s that is equal to 28.8 km/h. This speed value is higher than conventional range for linear motors motion. Figure 10 shows the reference and actual speed of LIM that is tracked by DTFC method preciously. The settling time is equal to 0.65 sec that is good for this range of speed. Achieving reference value without any oscillation and ripple is evident.

For used LIM according to parameters shown in Table 2, 0.25 wb is selected as the reference value of motor flux that Figure 11 shows the actual flux of motor. The LIM can track the reference value at 0.21 sec that illustrates fast settling time and high dynamic response. One of the most important features of DTFC is reducing ripple amplitude. Figure 12 shows the zoomed view of flux. Maximum ripple amplitude is less than 0.002 wb that is equal to less than 0.8% of amplitude.

With selecting d-axis of d-q reference frame in direction of flux motor, according to Figure 13, the flux amplitude of motor in q-axis direction will be equal to zero and whole flux will be created in d-axis direction. The three-phase fluxes show in Figure 14 that after achieving reference speed at $t = 0.7$ sec, all parameters have constant value. The thrust of motor to generate desired speed is shown in Figure (15). The maximum amplitude of thrust is less than 100 N that illustrate the capability of controller to control roughly high speed LIM with low thrust ripple and oscillation.

In order to create the flux and thrust of motor according to related references, the current that motor consumed through grid is shown in Figure 16. Figures 16(a) and 16(b) show the current in d-q axis and Figure 16(c) shows three-phase currents respectively. As mentioned earlier, the end-effect phenomenon causes destructive effect in the performance of LIM. By using Equations (1) and (2), Figure 17 shows the amplitude of end-effect phenomenon that is relevant to linear speed and varies with speed changes. After achieving reference speed amplitude by motor, the changes of $f(Q)$ is constant.
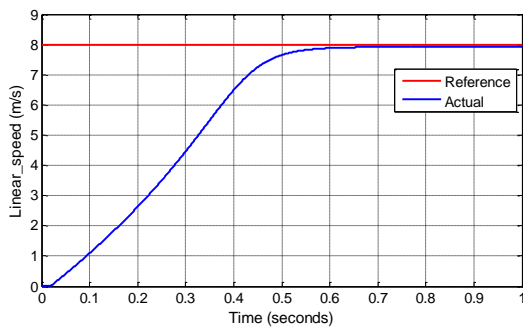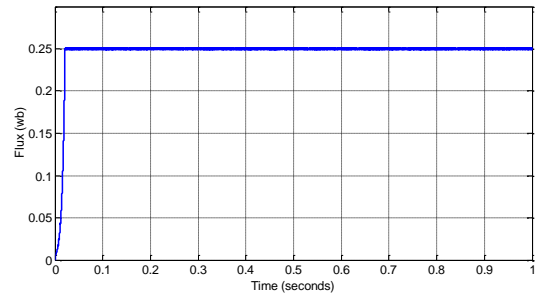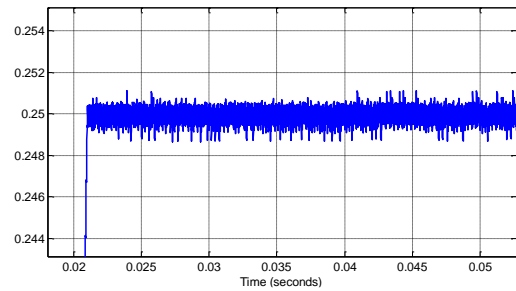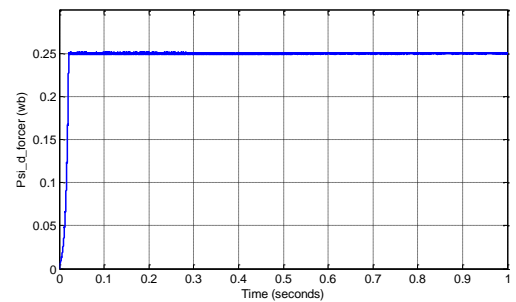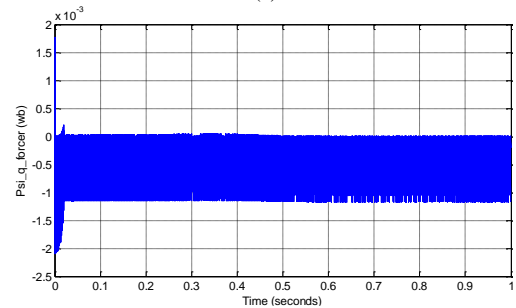

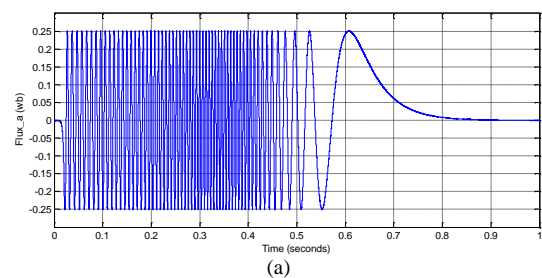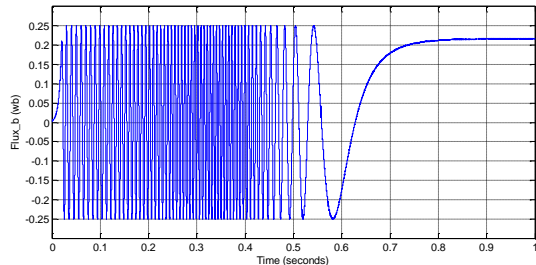Figure 11. The reference flux amplitude

Figure 12. Zoomed view of flux amplitude

(a)

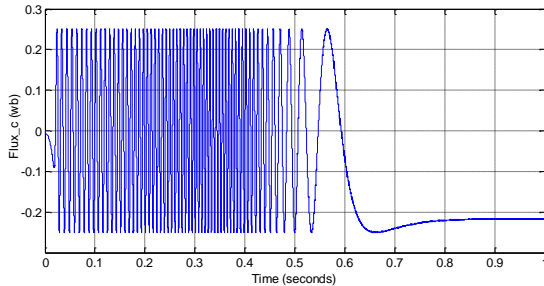

(b)

Figure 13. The reference flux of FORCER
(a) d-axis   (b) q-axis

(a)

Figure 5. The linear speed of motor

(b)

(c)

Figure 14. The three phase of reference flux
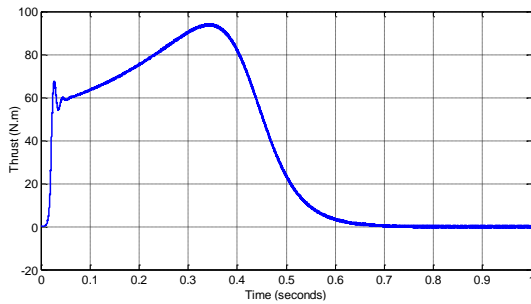(a) phase a   (b) phase b   (c) phase c
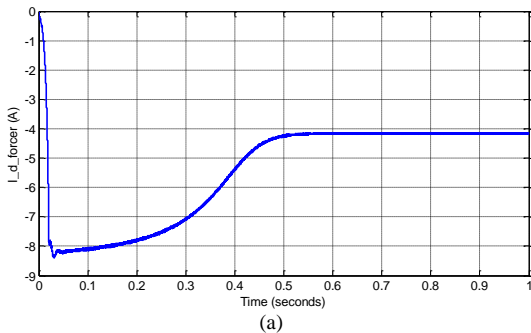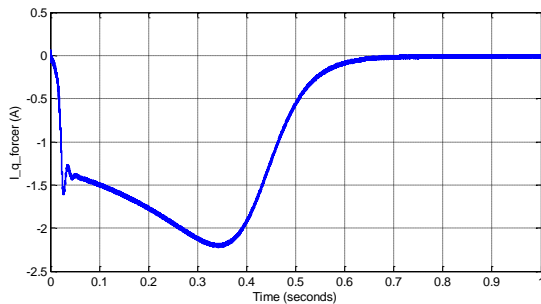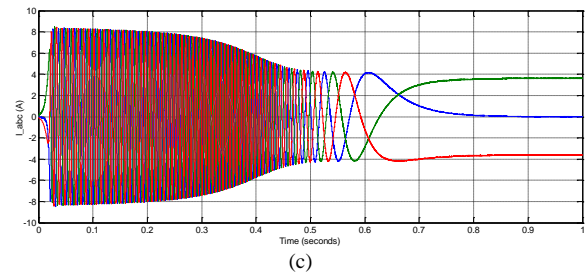

Figure 6. The thrust of motor

(a)

(b)

(c)

Figure 7. The current of FORCER
(a) d-axis   (b) q-axis   (c) abc

Figure 8. The $f(Q)$ function

Table 2. LIM motor parameters

R_s (Ω)	1.3	D (m)	0.308
R_r (Ω)	2.66	Pole pitch	0.066
L_s (H)	0.06	Number of pole	4
L_r (H)	0.0451	M (kg)	4.5
L_m (H)	0.0376	Motor Width (m)	0.33

VI. CONCLUSIONS

In this paper, speed control of LIM using direct thrust force control (DTFC) method based on dynamic model of LIM with considering end-effect phenomenon is presented. In this control method, flux and thrust relations by considering end-effect are rewritten. Using these equations, thrust force and flux values are estimated for using in controller. Because of the important role of PI coefficients in its operation, the coefficients are determined using MALAB optimization function. The DTFC method improved the ripple of motor characteristics such as flux and thrust which were confirmed by simulation results. Also in the control method DTFC, the end-effect hasn't any destructive effect on speed control, thrust and flux distortion.

REFERENCES

[1] G. Mino Aguilar, A.M. Dominguez, M.R. Alvarez, R. Cortez, G. Muoz, F. Guerrero, S. Maya, M. Rodriguez, F. Portillo, H. Azucena, "A Direct Torque Control for a PMSM", Electronics, 20th International Conference on Communications and Computer (CONIELECOMP), pp. 260-264, 22-24 Feb. 2010.

[2] E.F. da Silva, C.C. Dos Santos, J.W.L. Nerys, "Field Oriented Control of Linear Induction Motor Taking Into Account End-Effects", 8th IEEE International Workshop on Advanced Motion Control 2004 AMC'04, pp. 689-694, 25-28 March 2004.

[3] J. Zhao, Y. Zhongping, L. Jianqiang, T.Q. Zheng, "Indirect Vector Control Scheme for Linear Induction

Motors Using Single Neuron PI Controllers with and Without the End Effects", 7th World Congress on Intelligent Control and Automation (WCICA 2008), pp. 5263-5267, 25-27 June 2008.

[4] A.Z. Bazghaleh, M. Naghashan, H. Mahmoudimanesh, M. Meshkatoddini, "Effective Design Parameters on the End Effect in Single-Sided Linear Induction Motors", Methods, Vol. 5, p. 9, 2010.

[5] A. Memmedov, T. Abbasov, M. Seker, "Instantaneous Direct Control of Both Magnetic Flux and Output Power of Induction Motors Using Fuzzy Logic Controller", International Journal on Technical and Physical Problems of Engineering (IJTPE), Iss. 11, Vol. 4, No. 2, pp. 76-80, June 2012.

[6] Y.S. Lai and J.H. Chen, "A New Approach to Direct Torque Control of Induction Motor Drives for Constant Inverter Switching Frequency and Torque Ripple reduction", IEEE Transactions on Energy Conversion, Vol. 16, pp. 220-227, 2001.

[7] D. Casadei, F. Profumo, G. Serra, A. Tani, "FOC and DTC: Two Viable Schemes for Induction Motors Torque Control", IEEE Transactions on Power electronics, Vol. 17, pp. 779-787, 2002.

[8] A. Memmedov, T. Abbasov, M. Seker, "Some Aspects of the Magnetic Field Distribution Problems of Linear Induction Motor", International Journal on Technical and Physical Problems of Engineering (IJTPE), Issue 19, Vol. 6, No. 2, pp. 54-56, June 2014.

[9] R.H. Manno, E.G. Diez, "Direct Force Control for a Three-Phase Double-Sided Linear Induction Machine with Transverse Magnetic Flux", 28th Annual Conference on IECON 02, Industrial Electronics Society, IEEE 2002, Vol. 4, pp. 2826-2831, 5-8 Nov. 2002.

[10] G.G. Kang, K. Nam, "Field-Oriented Control Scheme for Linear Induction Motor with the End Effect", IEE Proceedings Electric Power Applications, Vol. 152, No. 6, pp. 1565-1572, 4 Nov. 2005.

[11] J. Thomas, A. Hansson, "Speed Tracking of a Linear Induction Motor-Enumerative Nonlinear Model Predictive Control", IEEE Transactions on Control Systems Technology, Vol. 21, No. 5, pp. 1956-1962, Sept. 2013.

[12] D. Hall, J. Kapinski, M. Krefta, O. Christianson, "Transient Electromechanical Modeling for Short Secondary Linear Induction Machines", IEEE Transactions on Energy Conversion, Vol. 23, No. 3, pp. 789-795, Sept. 2008.

[13] C.I. Huang, H.K. Cheng, H.H. Chiang, K. Kuang Yang, L. Tsu Tian, "Adaptive Fuzzy Sliding Mode Control of Linear Induction Motors with Unknown end Effect Consideration", International Conference on Advanced Mechatronic Systems (ICAMechS), pp. 626-631, 18-21 Sept. 2012.

[14] X. Wei, Z. Jian Guo, Zh. Yongchang, L. Zixin, L. Yaohua, W. Yi, G. Youguang, L. Yongjian, "Equivalent Circuits for Single-Sided Linear Induction Motors", IEEE Transactions on Industry Applications, Vol. 46, No. 6, pp. 2410-2423, Nov.-Dec. 2010.

BIOGRAPHIES

Hamed Shadabi was born in Ardebil, Iran. He received the B.Sc. degree in Power Engineering from University of Mohaghegh Ardabili, Ardabil, Iran in 2012. He is currently studying the M.Sc. degree in Faculty of Electrical Engineering at University of Tabriz, Tabriz, Iran. His current research interests include electrical drives of electrical machines, electrical and hybrid vehicles, power electronics applications.

Amin Rahnama Sadat was born in Tabriz, Iran. He received the B.Sc. degree in Power Engineering with the first rank honor in 2011 and the M.Sc. degree in Electrical Machines and Drives with the first rank honor in 2014 from University of Tabriz, Tabriz, Iran. His research interests include electric drives, liner motors, power electronic applications and electric and hybrid electric vehicle drives.

Ali Pashaei was born in Tabriz, Iran. He received the B.Sc. degree in Electrical Engineering in 2011 and the M.Sc. degree in Electrical Engineering from Gazi University, Ankara, Turkey, in 2013. He is currently Ph.D. student in Electrical Engineering in Gazi University. From 2012 he is working as a Research Assistant in Gazi University. His research interests are in the areas of renewable energy sources, energy conversion systems, power electronics and electrical machines.

Mohammad Bagher Banna Sharifian was born in Tabriz, Iran in 1965. He studied Electrical Power Engineering at the University of Tabriz, Tabriz, Iran. He received the B.Sc. and M.Sc. degrees in 1989 and 1992, respectively from the University of Tabriz. In 1992, he joined the Electrical Engineering Department of the University of Tabriz as a lecturer. He received the Ph.D. degree in Electrical Engineering from the same University in 2000. In 2000, he rejoined the Electrical Power Department of Faculty of Electrical and Computer Engineering of the same university as Assistant Professor. He is currently a Professor of the mentioned department. His research interests are in the areas of design, modeling and analysis of electrical machines, transformers, electric drives, liner electric motors, and electric and hybrid electric vehicle drives.